

Design, Fabrication, and Micro-Reflectance Measurement of a GaAs/AlAs-Oxide Antireflection Film

Yeonsang PARK, Joong-Seon CHOE* and Heonsu JEON†

School of Physics and Inter-university Semiconductor Research Center, Seoul National University, Seoul 151-747

(Received 21 July 2001, in final form 11 January 2002)

We have designed and fabricated a double-layer antireflection (AR) film by selective oxidation of an epitaxially grown GaAs/AlAs heterostructure. The method presented in this work has the advantage that it is much simpler in processing than the conventional AR coating method. Furthermore, the fabrication steps for the AR films are fully compatible with the standard monolithic semiconductor device processing technology so that the films can be easily and economically manufactured. The reflectance of the fabricated AR films was measured using a micro-reflectance measurement setup based on a 2×1 fiber coupler, which offered a spatial resolution on the order of the fiber core diameter. The measured reflectance showed a minimum value as low as 0.0033 at a wavelength of 1064 nm, and the 1 % reflectance bandwidth was measured to be 23 nm.

PACS numbers: 42.79.Wc, 78.66.Fd, 78.66.Nk

Keywords: AlAs, Oxidation, Antireflection, Micro-reflectance

I. INTRODUCTION

In recent years, oxide layers formed by wet thermal oxidation of AlGaAs epitaxial layers with high Al-composition have found their usefulness in various optoelectronic device applications. For example, the excellent insulating property of the oxide layers provides a convenient scheme of current confinement, useful for both edge and surface emitting lasers [1,2]. In addition, the low refractive indices of the oxide materials allow their use in optical elements. Upon selective lateral oxidation, an epitaxially grown $\text{Al}_x\text{Ga}_{1-x}\text{As}/\text{Al}_y\text{Ga}_{1-y}\text{As}$ multilayer structure can be converted to a highly reflecting (HR) distributed Bragg reflector (DBR) mirror. In this case the total layer pair number can be substantially reduced from that of a conventional semiconductor DBR mirror, owing to the enhancement in index contrast [3]. Very recently, Knopp *et al.* proposed the use of oxidized AlGaAs layers in anti-reflection (AR) coatings and experimentally demonstrated a few AR coating structures [4]. Compared to HR coatings, AR coatings are generally quite stringent in both design and fabrication, despite their structural simplicity, because the spectral position and the absolute value of the minimum reflectance are very sensitive functions of the layer thickness and the refractive indices of the constituent materials. In this context, the conversion of epitaxially grown single-crystal AlGaAs to a lower index dielectric could be highly advan-

tageous over the conventional direct deposition methods for optical materials by means of electron-beam evaporation or sputtering. With the oxidation method, control of refractive index, as well as the layer thickness, is much more reproducible.

In this work, we designed and fabricated the simplest and most reliable oxidized AR film based on the GaAs/AlAs system. The epilayer consisted only of binary materials, GaAs and AlAs, so that the growth was straightforward and the resultant films were highly reproducible. Also, the GaAs layer was designed to be on top of the AlAs layer, which is very important since the oxidized AlAs layer is quite fragile and porous so that its physical properties are subject to change once exposed to the air. For optical probing of the AR film over a small area, we implemented a simple micro-reflectance measurement setup using a 2×1 optical fiber coupler.

II. AR COATING THEORY

Throughout this work, the spectral position of the reflectance minimum of the AR film is nominally aimed at 980 nm, the emission wavelength of the pump laser source for an Er-doped fiber amplifier (EDFA). It is well known that the simplest AR film structure consists of a single layer with its refractive index and thickness being $n = \sqrt{n_0 n_m}$ and $t = \lambda/4n$, where n_0 and n_m are the indices of the incident medium and the substrate while λ is the wavelength of the light. Since the AR layer index n seldom satisfies this index matching condition for a given

*Present address: Basic Research Lab., Electronics and Telecommunications Research Institute, Taejeon 305-600

†E-mail: hsjeon@phya.snu.ac.kr

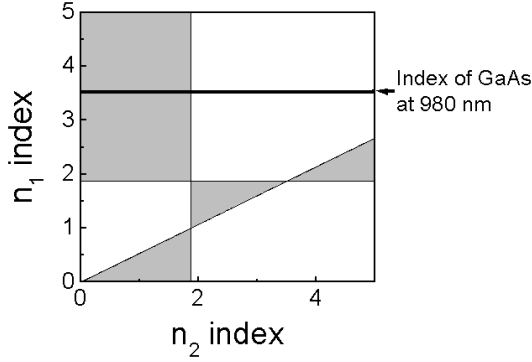


Fig. 1. Index diagram for a double-layer anti-reflection (AR) film. The gray region indicates the index ranges for two constituents from which anti-reflection film can be constructed.

incident medium and substrate material, here we focus on a double-layer AR structure. In this scheme, one can design AR films by simply adjusting the layer thickness without having to actively control the material indices.

By applying the transfer matrix formalism [5] to a double layer system and equating the resultant reflectance to zero, one can obtain two equations that determine the layer thickness:

$$\begin{aligned} \tan^2 \delta_1 &= \frac{(n_m - n_0)(n_2^2 - n_0 n_m) n_1^2}{(n_1^2 n_m - n_0 n_2^2)(n_2^2 - n_0 n_m)}, \\ \tan^2 \delta_2 &= \frac{(n_m - n_0)(n_0 n_m - n_1^2) n_2^2}{(n_1^2 n_m - n_0 n_2^2)(n_2^2 - n_0 n_m)}, \end{aligned} \quad (1)$$

where $\delta_i = 2\pi n_i d_i / \lambda$ is the phase factor of a normally propagating wave, and n_0 , n_m , and n_i are the indices of the air, the substrate, and the i -th layer, respectively, while d_i is the thickness of the i -th layer. In our convention, $i=1$ is the outermost layer exposed to the air, and $i=2$ is the inner layer adjacent to the substrate. For solutions to exist, the right-hand sides of the above equations must be positive, which is equivalent to

$$(n_2^2 - n_0 n_m)(n_1^2 n_m - n_0 n_2^2)(n_0 n_m - n_1^2) \geq 0. \quad (2)$$

This inequality can be summarized in a pictorial index diagram. If GaAs is the substrate material ($n_m=3.5$ at 980 nm), the index diagram for n_1 and n_2 is as shown in Fig. 1. If we further require that the $i=1$ layer material is also GaAs ($n_1=3.5$), the $i=2$ material should have an index less than 1.87, which is indicated by the horizontal line in Fig. 1. This requirement on n_2 is safely fulfilled by oxidized AlAs since its index is about 1.56 at 980 nm according to measurements of our own as well as of others [6,7]. Solving the equations in eq. (1) with those material choices determines d_1 and d_2 uniquely, and they are 83 nm and 153 nm, respectively. At this point, it should be noted that both GaAs and oxidized AlAs are transparent at the target wavelength of 980 nm and beyond. Further simulations of the reflectance spectrum with the above parameters reveal that the bandwidth for 1 % reflectance is about 31 nm.

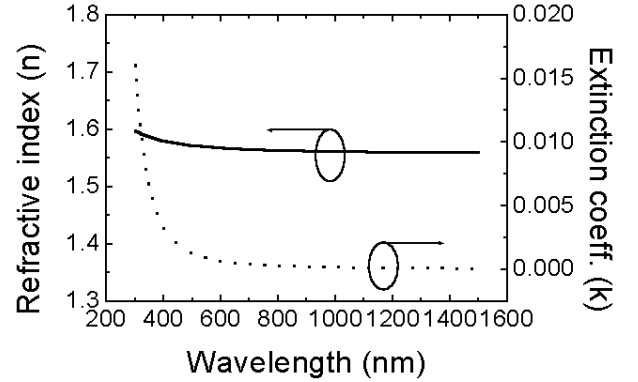


Fig. 2. Refractive index (n) and extinction coefficient (k) of the oxidized AlAs layer measured by using the spectroscopic ellipsometric technique. The solid and the dotted lines represent n and k , respectively. Note that k is negligibly small at a wavelength around 1 μm , indicating that the oxidized AlAs is free from absorption.

III. EXPERIMENT

1. Fabrication of AR Films

A GaAs/AlAs double-layer structure was grown on a (001)-oriented GaAs substrate by using atmospheric-pressure metal-organic chemical-vapor-deposition (AP-MOCVD). Prior to the actual AR structure growth, the material deposition rate was carefully calibrated for layer thickness control. Special care was taken for the AlAs layer in order to take into account the volume contraction after oxidation [8]. The information on the oxidized AlAs layer thickness, as well as its full dispersions of the refractive indices (both real and imaginary parts), was obtained from a separate single AlAs layer growth, oxidation, and spectroscopic ellipsometer measurement. We confirmed that after oxidation approximately a 20 % reduction in thickness exists, consistent with other results. The measured refractive indices of the oxidized AlAs film are graphically displayed in Fig. 2. All these preliminary data were then fed back into the AR film design.

To prevent surface decomposition of GaAs during thermal oxidation, we deposited a 100-nm-thick SiN passivation layer on top of the MOCVD-grown epilayer structure by using plasma-enhanced chemical-vapor deposition (PECVD). Then, a series of 120- μm -wide SiN stripes were defined using the standard photolithography, and the epi-structure in the remaining exposed area was dry-etched until the substrate was reached. After removing the photoresist mask, the sample was oxidized fully in an oxidation chamber. The full lateral oxidation over the 120- μm -wide stripe took over an hour at the chamber temperature of 420 $^\circ\text{C}$. Finally, the SiN passivation layer was removed by dry etching. The fabricated AR film structure is schematically illustrated in Fig. 3.

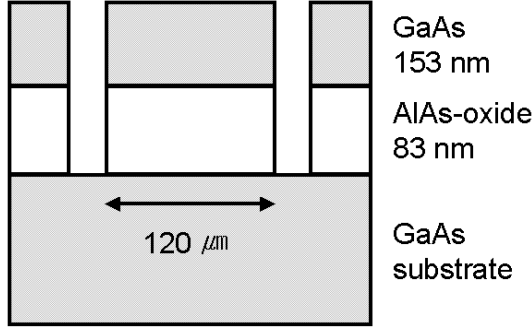


Fig. 3. Schematically drawn double-layer AR film structure with the layer thickness designed for minimum reflectance at 980 nm.

2. Reflectance Measurement

To measure the reflectance of a fabricated AR film in which the structure is segmented for oxidation, we need a special apparatus whose spatial resolution is less than at least the stripe width. For this purpose, we have made a simple reflectance measurement setup using a 2×1 fiber coupler. Since the system is based on optical fibers, its spatial resolution is inherently on the order of the fiber core diameter. The 2×1 fiber coupler greatly simplifies the reflectance measurement, replacing the beam-splitter, fiber couplers, and objective lenses for beam collimation/focusing from a conventional fiber-based optical measurement setup. Our reflectance setup is composed of a light source, a fiber coupler, a sample stage, and an optical spectrum analyzer, as schematically illustrated in Fig. 4. A tungsten halogen lamp is used as a white light source, and the optical signal reflected from a sample is directly input into an optical spectrum analyzer through a fiber.

In the actual measurement, we first measure the intensity spectrum for the light reflected from a reference sample whose reflectance is known. In this experiment, we choose a gold mirror as the reference since it reflects near-infrared light almost completely. Then, the same

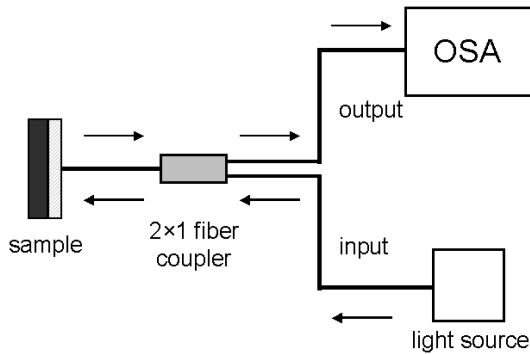


Fig. 4. Block diagram of the micro-reflectance measurement setup.

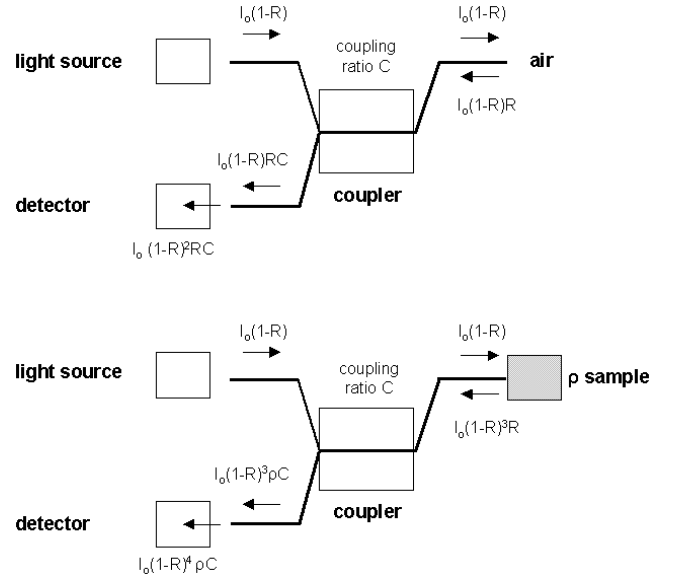


Fig. 5. Block diagrams for reflectance measurement analysis. I_0 represents the input power whereas R , C , and ρ are the Fresnel reflectance of the optical fiber, the coupling ratio of the 2×1 fiber coupler, and the reflectance coefficient of the sample, respectively.

measurement is repeated for a sample. The sample-to-reference intensity ratio gives the reflectance spectrum of the sample on an absolute scale after some numerical manipulations [9].

Now, let us derive the equation that relates what we measure experimentally to the actual reflectance. The analysis procedures are schematically shown in Fig. 5. We define the incident power and the background reflectance at the interface of the fiber tip and the air as I_0 and R , respectively. In the absence of a sample, a fraction $1 - R$ of the incident light power I_0 is transmitted into the input port. After it travels through the coupling region, this light reaches the end of the fiber. Then, the fraction R of the traveled light $I_0(1 - R)$ is reflected back at the end of the fiber. After the light returns, it passes through the coupler region and is divided according to coupling coefficient C . Finally, light with intensity $I_{air} = I_0(1 - R)^2 RC$ is transmitted into the detector. A similar analysis can be done in the presence of a sample with reflectance ρ , and the resulting signal intensity that reaches the detector is $I = I_0(1 - R)^4 \rho C$. When we define the quantity A as the intensity ratio of a sample to the reference, it is given as

$$\begin{aligned}
 A &= \frac{I_{air} + I(\rho)}{I_{air} + I_{refer}(\rho_{refer} \cong 1)} \\
 &= \frac{I_0(1 - R)^2 RC + I_0(1 - R)^4 \rho C}{I_0(1 - R)^2 RC + I_0(1 - R)^4 \rho_{refer}(\cong 1)C} \\
 &= \frac{R + (1 - R)^2 \rho}{R + (1 - R)^2}. \tag{3}
 \end{aligned}$$

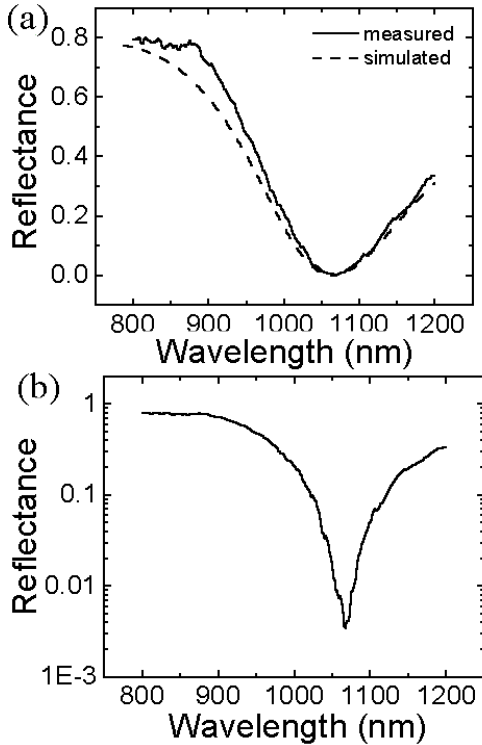


Fig. 6. (a) Reflectance spectrum of the double-layer AR film measured using the micro-reflectance measurement setup with a 2×1 fiber coupler. The dashed line indicates the simulated reflectance. (b) The same reflectance spectrum, but represented on a logarithmic scale.

By rearranging the above equation, we obtain

$$\rho = \frac{A(R + (1 - R)^2) - R}{(1 - R)^2}. \quad (4)$$

IV. RESULTS

We measured the signal intensity reflected from a fabricated AR film structure by using the fiber-coupler-based reflectance measurement setup. During the measurements, we paid special attention to the air gap between the sample and the fiber tip since it could produce run-to-run fluctuations in the measurements, depending on the gap distance. Our strategy to overcome this potential problem was to minimize the air gap by moving the fiber tip until it gently touched the sample surface. In this way, we could make the geometrical configuration reasonably identical every time and, therefore, ensure the reproducibility. Since in this approach the air gap at the measurement end is estimated to be less than $10 \mu\text{m}$ whereas the core diameter of the multimode fiber used in the experiment is $62.5 \mu\text{m}$, optical coupling loss should be practically negligible, as implicated by Eqs. (3) and (4).

Figure 6(a) illustrates the measured reflectance spectrum on a linear scale after data conversion as outlined in the previous section. The fabricated AR film structure was designed to consist of a 153-nm-thick GaAs layer and an underlying 82-nm-thick AlAs oxide layer. Although the reflectance minimum was designed to be at 980 nm, the measured minimum was shifted to 1064 nm. We attribute this result to the initial calibration error in growth rate and the spatial variation in layer thickness, the latter being an inevitable problem with our research-purpose small MOCVD reactor that accommodates only one $1\times 1 \text{ cm}^2$ piece of sample. Nonetheless, the reflectance was measured to be as low as 0.0033, and is expected to be even lower when optimized. For clear identification of the minimum reflectance value, the measured spectrum is redrawn on a logarithmic scale in Fig. 6(b). The bandwidth for which the reflectance is below 1 % is 23 nm, extending over the range from 1052 nm to 1075 nm. This bandwidth is slightly smaller than the value calculated theoretically. This discrepancy originates from the fact that the GaAs layer in the AR film becomes absorptive near and below its bandgap wavelength while the theoretical calculation assumes no optical absorption for either GaAs or the oxidized-AlAs. The GaAs bandgap appears in Fig. 6(a) as a small bump near 880 nm. The extended absorption tail below the GaAs bandgap reduces effectively the overall reflectance bandwidth. This argument is consistent with our observation that the discrepancy between the experimental and the theoretical results is severe only on the shorter wavelength side of reflectance dip where the bandgap effect plays a role.

V. CONCLUSION

We presented a method for forming a double-layer AR film by selectively oxidizing an AlAs layer from an appropriately designed epitaxial GaAs/AlAs heterostructure. The micro-patterned AR films were probed using a micro-reflectance measurement setup that we built based on a 2×1 fiber coupler. The measured reflectance spectrum was close to the theoretical simulation results, with a minimum reflectance of 0.0033, indicating the high optical quality of the GaAs/AlAs-oxide AR film.

The AR film and its fabrication method by selective oxidation have many advantages over the conventional AR coatings. Among others, the use of fully matured monolithic semiconductor processing techniques is the most powerful merit. The AR films presented in this paper are highly reproducible in principle and, therefore, should find many application possibilities, especially in conjunction with photonic devices whose light input/output is through the wafer surface, such as light-emitting-diodes and photodiodes. Also, the micro-reflectance measurement setup based on a 2×1 optical fiber coupler is easy to construct and use, and yet of-

fers good spatial resolution and reliability. Though not tried in this experiment, the spatial resolution of the reflectance measurement setup could be greatly improved by using a 2×1 coupler constructed of a single-mode fiber.

REFERENCES

- [1] J. M. Dallesasse and N. Holonyak, Jr., *Appl. Phys. Lett.* **58**, 394 (1991).
- [2] D. L. Huffaker, D. G. Deppe, K. Kumer and T. J. Rogers, *Appl. Phys. Lett.* **65**, 97 (1994).
- [3] M. H. MacDougal, H. Zhao, P. D. Dapkus, M. Ziari and W. H. Steiner, *Electron. Lett.* **30**, 1147 (1994).
- [4] K. J. Knopp, R. P. Mirin, K. A. Bertness, K. L. Silverman and D. H. Christensen, *J. Appl. Phys.* **87**, 7169 (2000).
- [5] H. A. Macleod, *Thin-film Optical Filters* (Adam Hilger Ltd, Bristol, 1986).
- [6] K. J. Knopp, R. P. Mirin, D. H. Christensen, K. A. Bertness, A. Roshko and R. A. Synowicki, *Appl. Phys. Lett.* **73**, 3512 (1998).
- [7] D. C. Hall, H. Wu, L. Kou, Y. Luo, R. J. Epstein, O. Blum and H. Hou, *Appl. Phys. Lett.* **75**, 1110 (1999).
- [8] S. Guha, F. Agahi, B. Pezeshki, J. A. Kash, D. W. Kisher and N. A. Bojarczuk, *Appl. Phys. Lett.* **68**, 906 (1996).
- [9] I. Tugendhaft, A. Bornstein, Y. Weisman and A. Hardy, *Appl. Opt.* **36**, 1297 (1997).